Co-sputtering strategy to construct robust sodiophilic interfaces for anode-less sodium metal batteries

Jiawen Dai, [a] Haoran Wang, [a] Rui Zhang, [a] Jin Wang, [a] Peiyu Wang, [b] Tian Qiu, [b], Haiyan Wang [a, b]*

[a]Hunan Provincial Key Laboratory of Chemical Power Sources

College of Chemistry and Chemical Engineering

Central South University

Changsha, 410083, P.R. China

[b] Guangdong DFP New Material Group Co. LTD, Shantou, 515064, P.R. China

E-mail: wanghy419@csu.edu.cn

Methods

Preparation of Cu@Bi and Cu@Cu-Bi foils

The uniform Cu@Bi and Cu@Cu-Bi foils were prepared in a facile method of magnetron sputtering. First, a piece of one-sided rough Cu foil with the size of 10 cm×10 cm was put into the equipment (TAILONG ElECTRONICS Sputter-100) as the substrate. Then, the chamber was evacuated to a pressure lower than 5.0×10^{-6} Pa before the magnetron sputtering. Ar atmosphere was used to clean the chamber at a flow rate of 100 sccm. The Bi coated Cu foil (Cu@Bi) was prepared under the power of 100 W RF for 3 min. The Cu and Bi coated Cu foil (Cu@Cu-Bi) was obtained through a 5 min sputtering process utilizing Cu target (at 200 W DC power) and Bi target (at 40 W RF power). At last, the prepared samples were cut into small round pieces with the diameter of 14 mm. Metal copper, bismuth targets with a diameter of 10 cm (99.99% purity) were purchased from ONA Targets Ltd. The one-sided rough Cu foil (12 μm) was purchased from Canrd Technology Co. Ltd.

Preparation of the cathode and electrolytes

$Na_4Fe_{2.91}(PO_4)_2(P_2O_7)$ cathode (NFPP) was purchased from Zhejiang Rich Power Technology Co. Ltd. The composition of the cathode slurry was 90wt% NFPP, 5wt% Super P and 5wt% poly(vinylidene fluoride) (PVDF). The electrode slurry was cast on Cu foil followed by a drying process under a vacuum. The mass loading of NFPP was about 10 mg cm^{-2}. The electrolyte was obtained by dissolving 0.9 M $NaPF_6$ (DoDoChem, battery grade) and 0.1 M $NaBF_4$ (ALADDIN, 99.9% metals basis) in diglyme (DoDoChem, battery grade).

Characterizations

In-situ X-ray diffraction (XRD) patterns were recorded using a Bruker D8 X-ray diffractometer with monochromatized Cu Kα radiation (wavelength = 1.5406 Å). Nondestructive-XRD results enabling avoidance of air contact were recorded using a Rigaku X-ray diffractometer. The scanning electron microscope (SEM, JSM-

7610FPlus) with non-destructive transfer capability was used to characterize the sodium plating and stripping morphology of the substrate. The cross-sectional SEM samples of the substrate after sodium deposition were obtained by cryo-focused ion beam processing. Optical microscopy (AOSVI M203-HD228S) equipped with an in-situ reaction device was used to observe the evolution of sodium deposition. Transmission electron microscopy (TEM, JEOL/JEM-F200) was used to characterize the crystal structure evolution after the plating/ stripping reaction. The spatial distribution of SEI composition at the substrate interface was obtained using time-of-flight secondary ion mass spectrometry combined with ion beam etching (TOF-SIMS, with non-destructive transfer device, Thermo scientific Scios 2 Hivac, TOFWERK, 30 keV Ga ion sputter gun).

Electrochemical measurements

Standard CR2032 coin cells were assembled in an argon-filled glove box and used for all the electrochemical measurements. The amount of electrolyte used for the coin cell was 120 μL. The sodium discs of 14 mm diameter was purchased from Canrd Technology Co. Ltd. Glass fibre (Whatman GF/A) plus Celgard C200 membrane was utilized as the separator of anode-less sodium metal battery (ASMB). The galvanostatic charge/discharge tests were performed using a Neware MIHW-200-160CH battery testing system. The ASMB did not perform any pre-treatment such as pre-sodiumation before cycling. During the cycling process, the AMSB was set to a charge cut-off voltage of 3.9 V and a discharge cut-off voltage of 1.5 V. The charge cut-off voltage of the Cu|| Na (or Cu@Bi|| Na and Cu@Cu-Bi|| Na) half-cells were set to 0.5 V (vs Na/Na^+). Electrochemical impedance spectroscopy (EIS) was measured in the frequency range from 0.01 kHz to 500 Hz with a voltage amplitude of 10 mV (AUTOLAB electrochemical workstation). The EIS of full cell was tested at full charge state (charged to 3.9 V).

Computational details

The first-principles calculations were conducted using generalized gradient approximation (GGA) and Perdew–Burke–Ernzerhof (PBE) exchange-correlation functional in DMol3 module of Materials Studio (version 2017) of Accelrys Inc. An all-electron numerical basis set with polarization functions (DNP basis set) with a basis file of 4.4 and a DFT-D method within the Grimme scheme was employed during calculating. The convergence tolerance was set to 1.0×10^{-5} eV per atom for energy, 3.0×10^{-2} eV $Å^{-1}$ for maximum force and 1.0×10^{-3} Å for maximum displacement. The simulation was taken using the substrate surface with a five-layer 3×3 supercell and releasable top three-layer atoms. The binding energy (Eb) was calculated by the following equation:

$$E_b = E_{total} - E_{sub} - E_{Na}$$

E_{total}, E_{sub} and E_{Na} represent the total energy of the surface adsorbed by Na atom, the energy of the surface and the energy of Na atom, respectively.

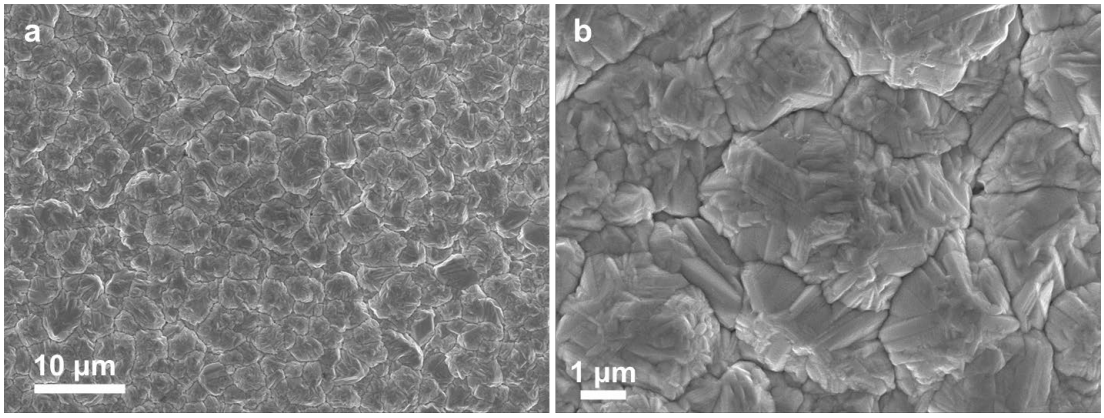

Figure S1. SEM images of Cu foil.

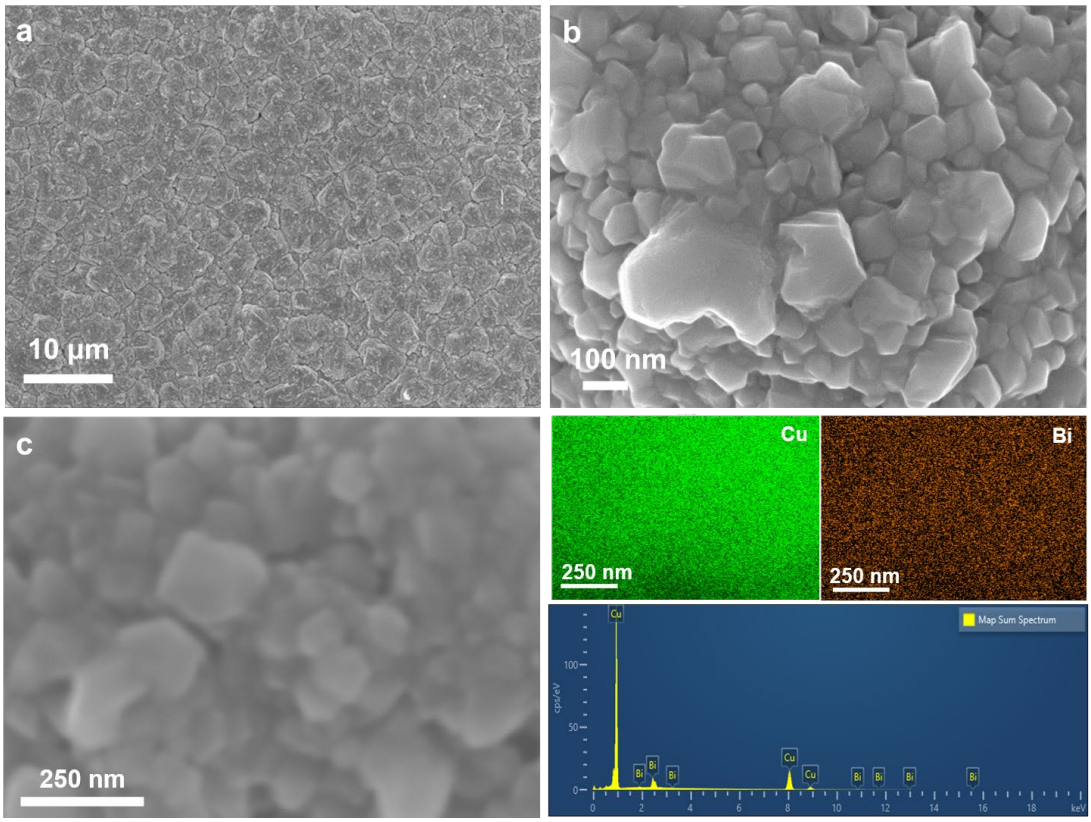

Figure S2. SEM images and the corresponding EDS mappings of Cu@Bi.

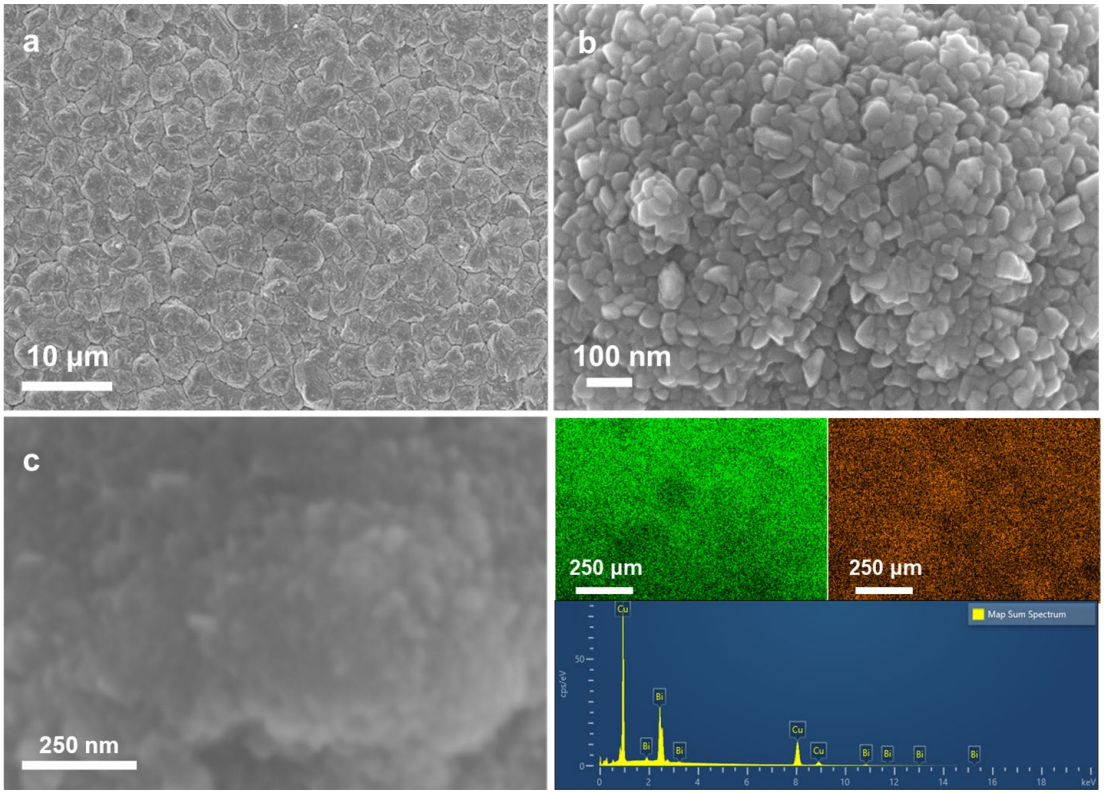

Figure S3. SEM images and the corresponding EDS mappings of Cu@Cu-Bi.

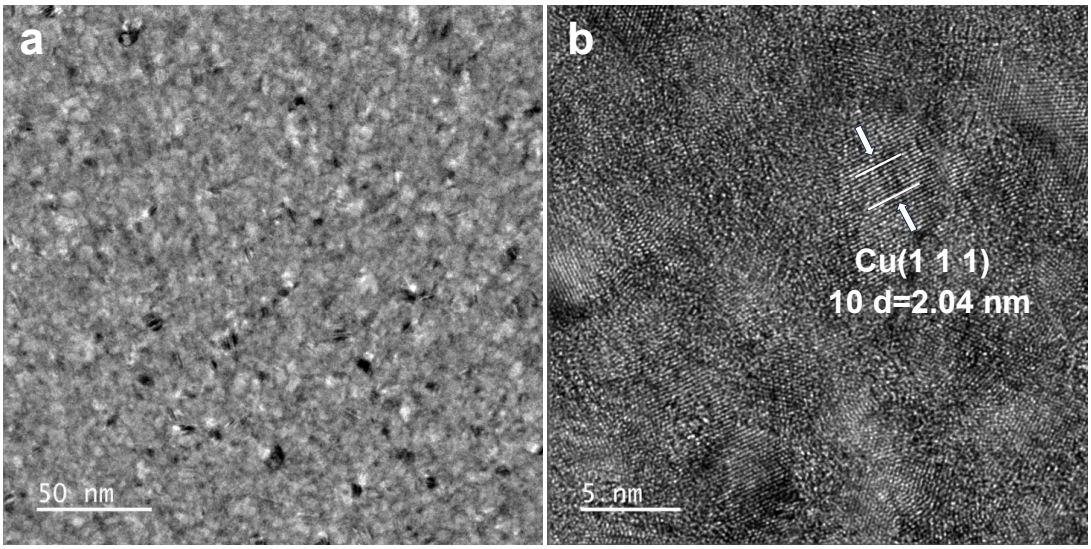

Figure S4. TEM and HRTEM images of copper and bismuth sputtered on molybdenum mesh.

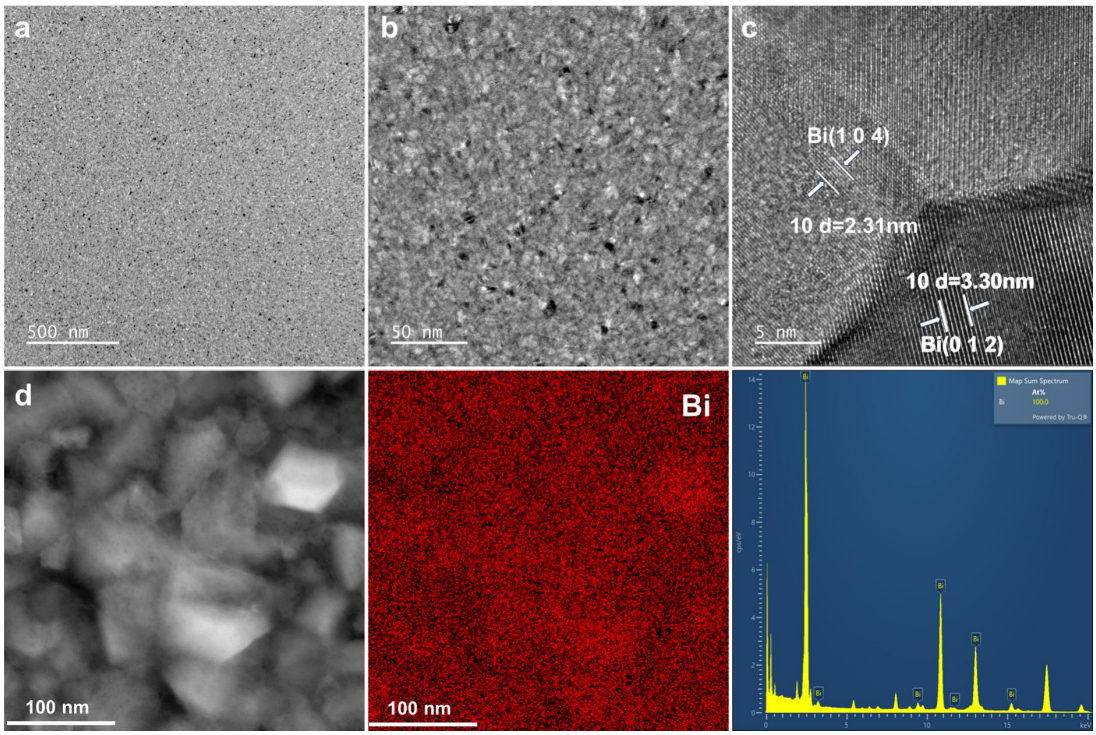

Figure S5. TEM, HRTEM and corresponding EDS mappings of bismuth sputtered on molybdenum mesh.

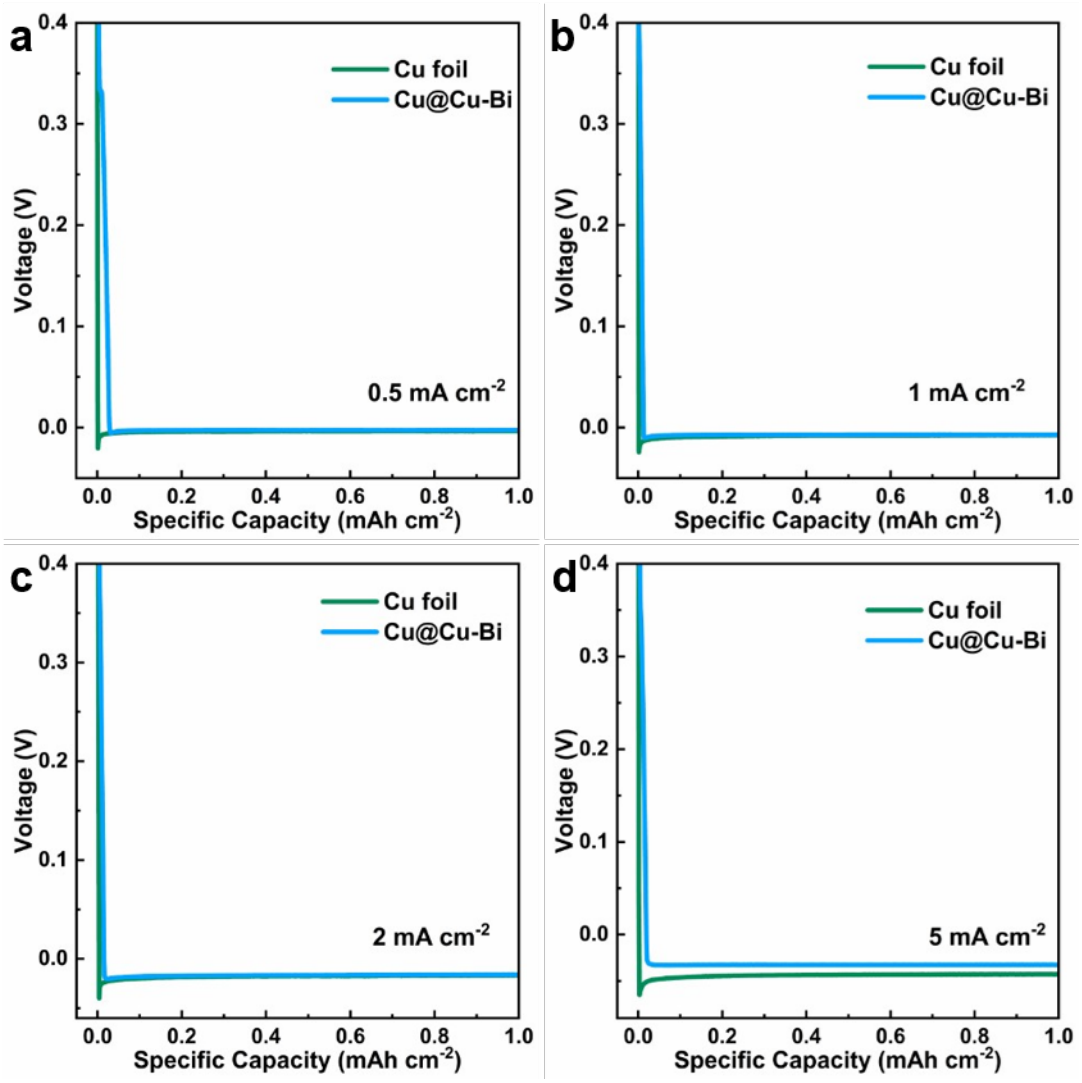

Figure S6. The initial capacity-voltage curves of Na|| Cu and Na|| Cu@Cu-Bi half-cells at different current densities.

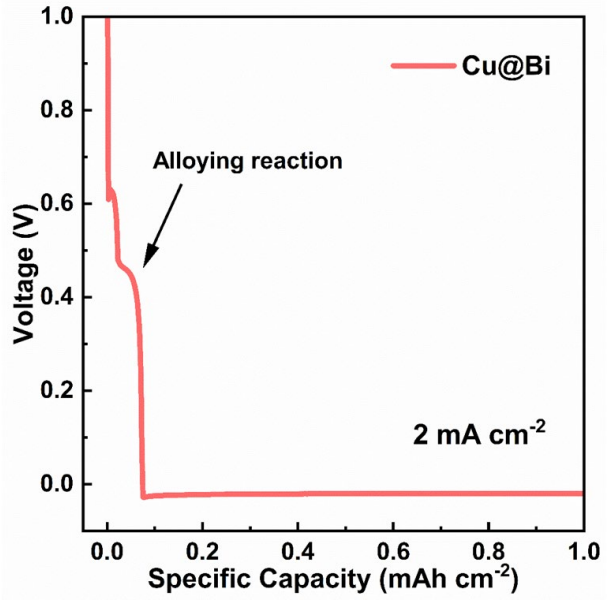

Figure S7. The initial capacity-voltage curve of Na|| Cu@Bi half-cells at 2 mA cm^{-2}.

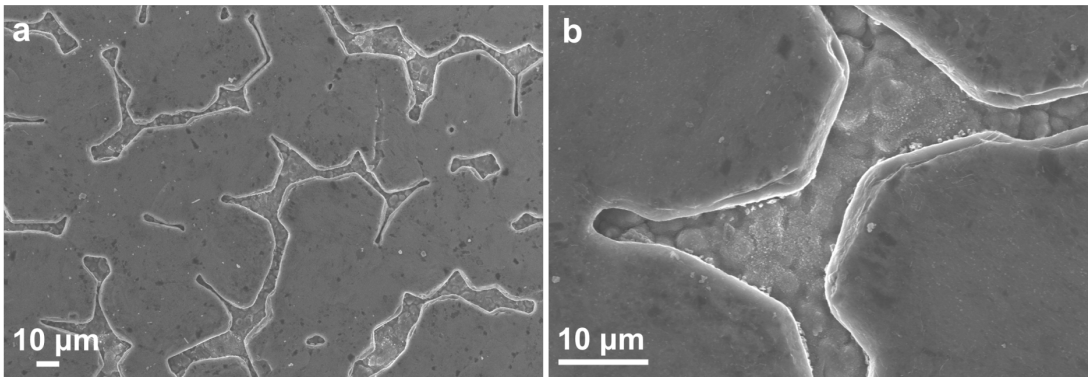

Figure S8. SEM images of sodium deposition on Cu foil at 1 mA cm^{-2} for 0.6 mAh cm^{-2}.

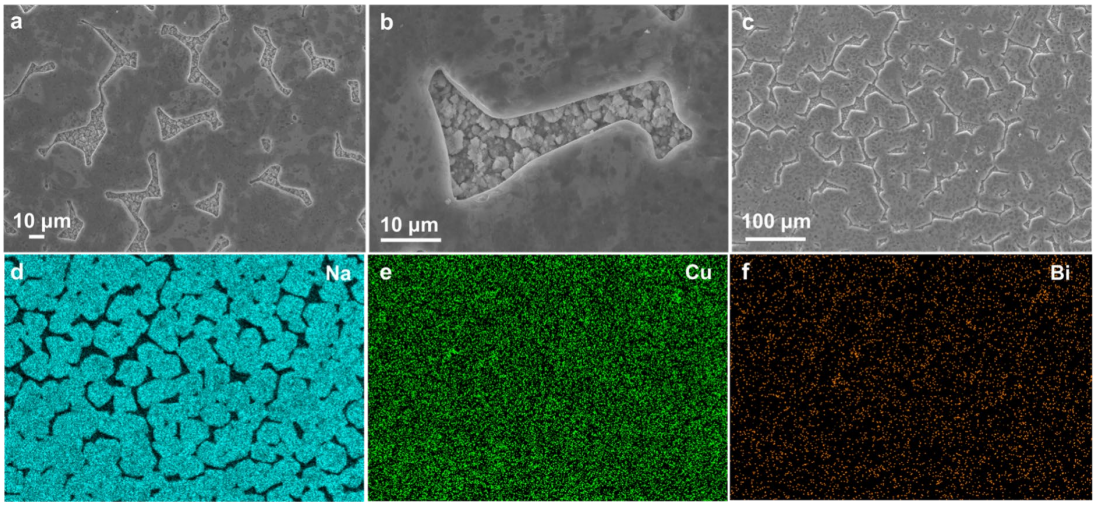

Figure S9. SEM images and the corresponding EDS mappings of sodium deposition on Cu@Cu-Bi at 1 mA cm^{-2} for 0.6 mAh cm^{-2}.

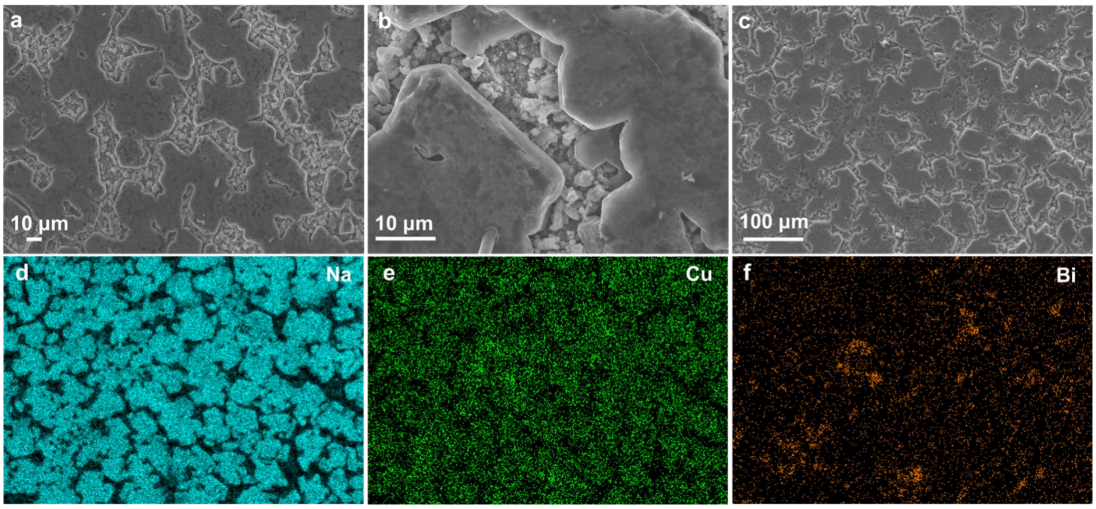

Figure S10. SEM images and the corresponding EDS mappings of sodium deposition on Cu@Bi at 1 mA cm^{-2} for 0.6 mAh cm^{-2}.

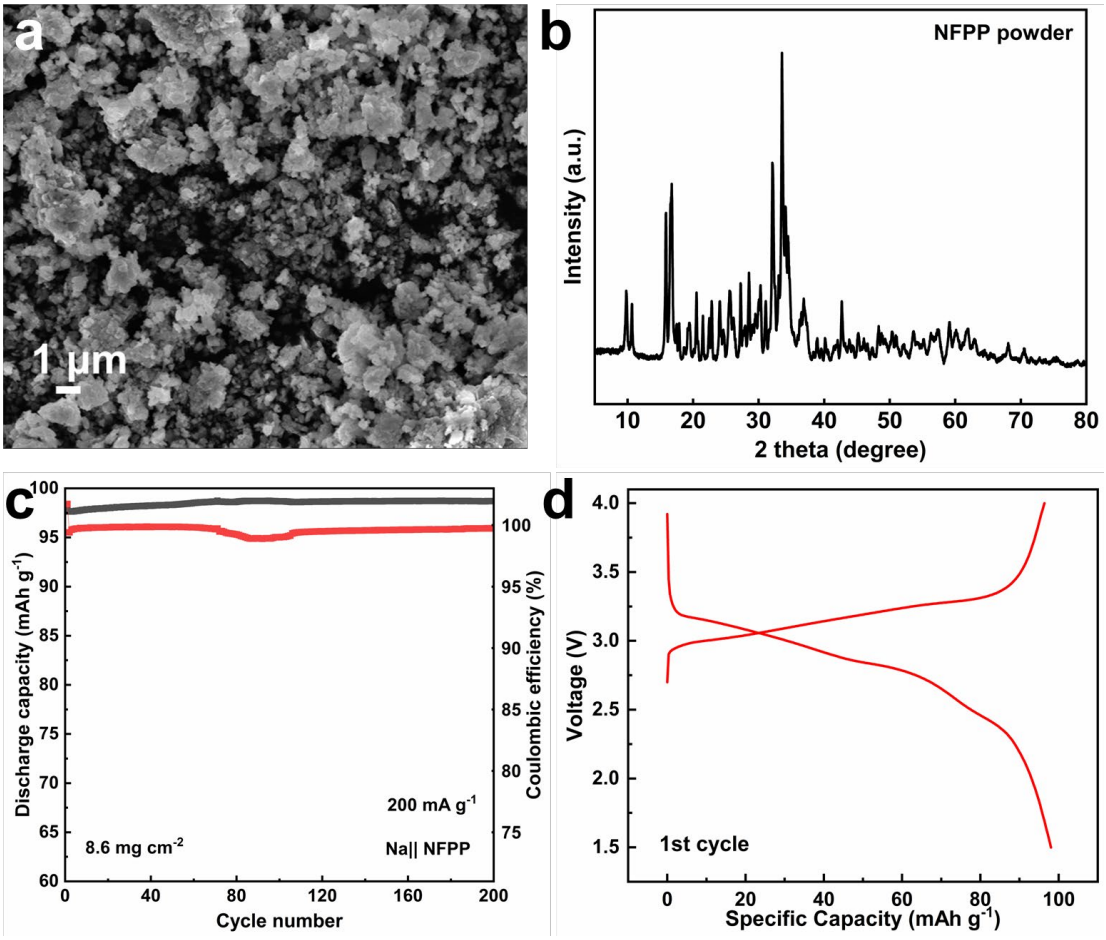

Figure S11. (a) SEM image and (b) XRD pattern of NFPP cathode, (c) cyclic performance and (d) the corresponding initial capacity-voltage curve of the Na||NFPP cell.

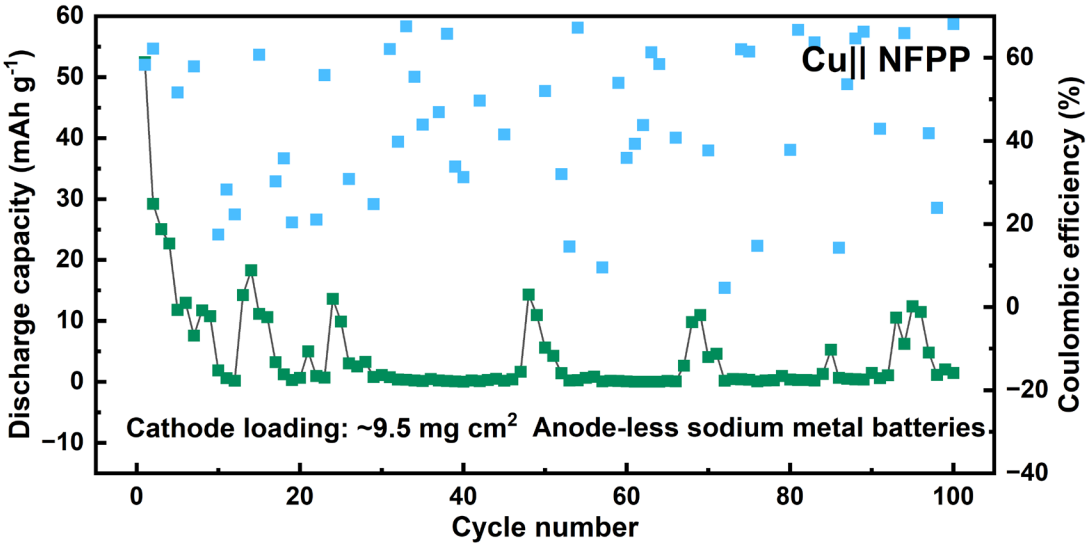

Figure S12. Cyclic stability of Cu|| NFPP anode-free cells.

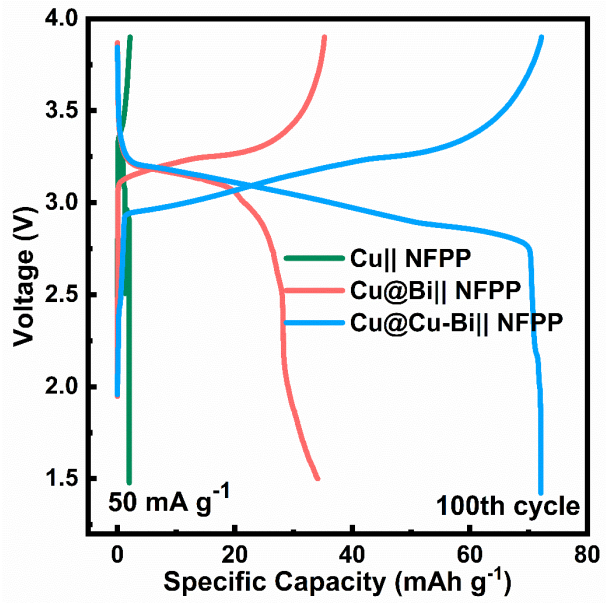

Figure S13. The capacity-voltage curves of Cu|| NFPP , Cu@Bi|| NFPP and Cu@Cu-Bi|| NFPP cells at 50 mA g^{-1}.

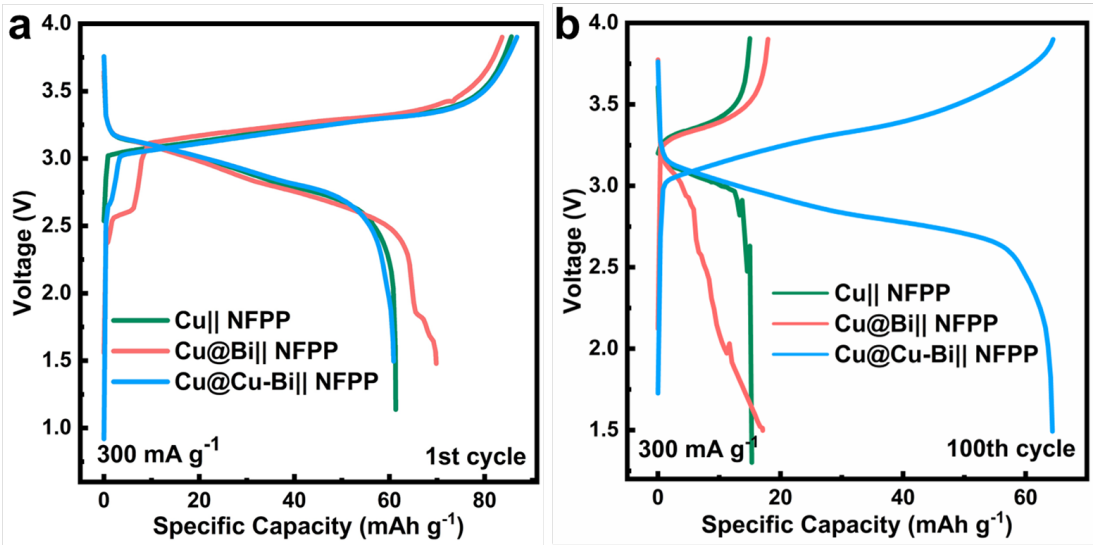

Figure S14. The capacity-voltage curves of Cu|| NFPP, Cu@Bi|| NFPP and Cu@Cu-Bi|| NFPP cells at 300 mA g^{-1}.

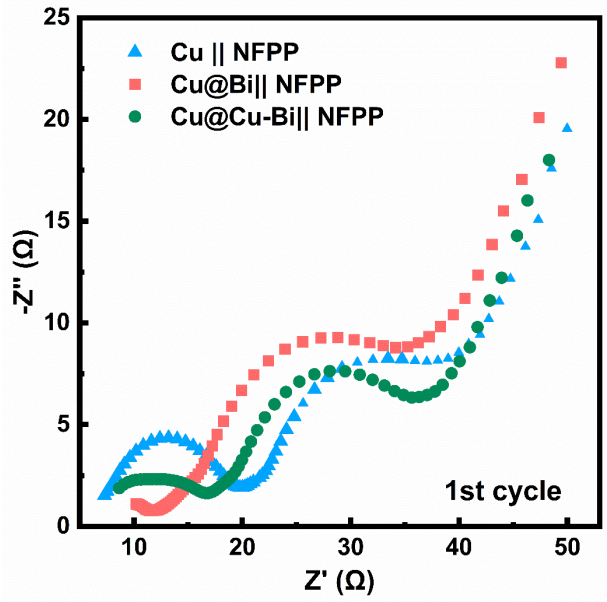

Figure S15. The EIS of Cu|| NFPP, Cu@Bi|| NFPP and Cu@Cu-Bi|| NFPP cells in the fully charged state for the first cycle.

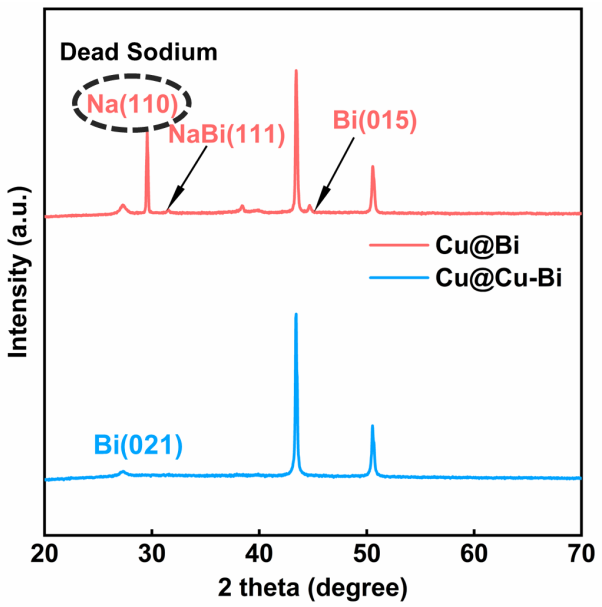

Figure S16. The anode-side XRD patterns of Cu|| NFPP and Cu@Cu-Bi|| NFPP cells in a fully discharged state after 50 cycles at 300 mA g^{-1}.

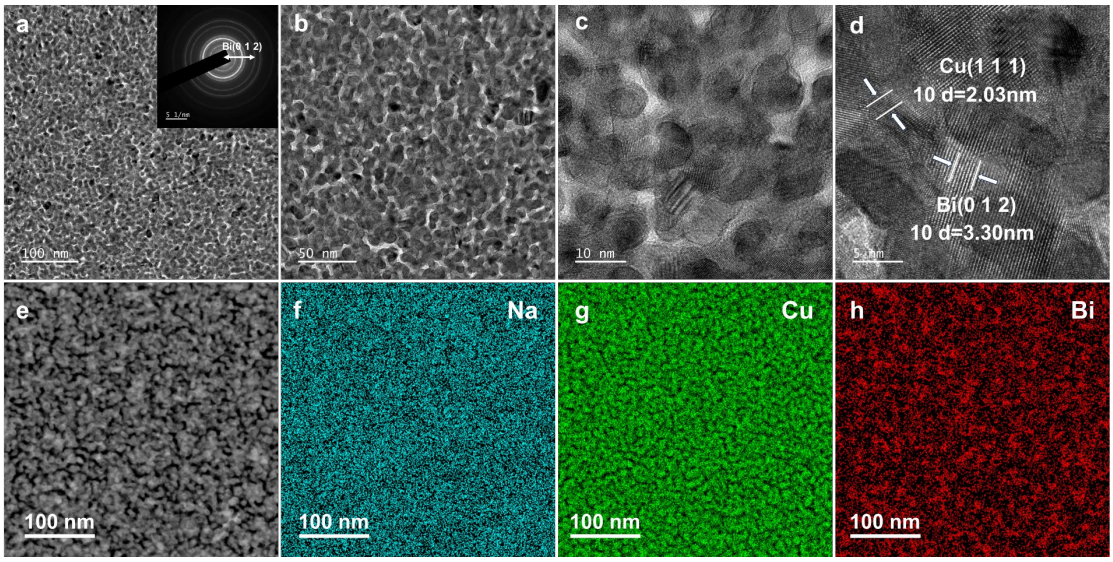

Figure S17. TEM images and the corresponding EDS mapping of copper and bismuth sputtered on molybdenum mesh after 50 cycles of sodium plating/stripping (in the stripped state).

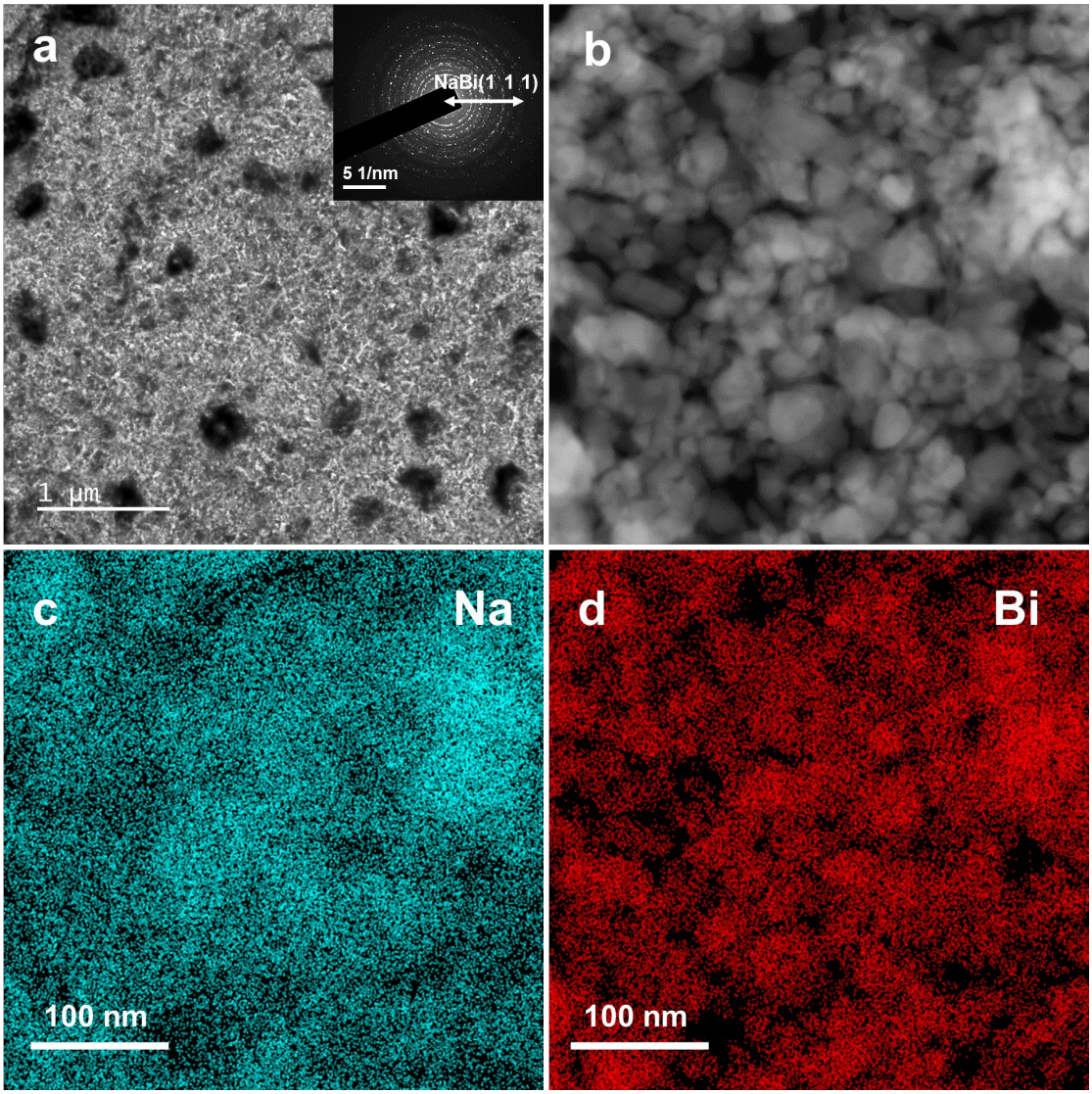

Figure S18. TEM images and the corresponding EDS mapping of bismuth sputtered on molybdenum mesh after 50 cycles of sodium plating/stripping (in the stripped state).

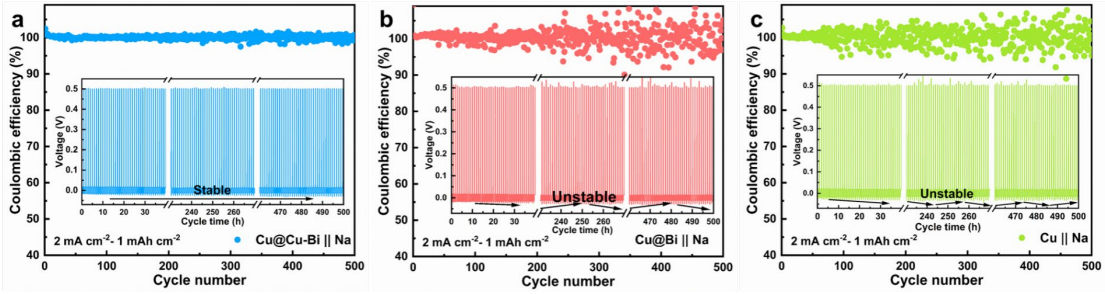

Figure S19. The voltage-time curves of the a) Cu@Cu-Bi|| Na, b) Cu@Bi|| Na and c) Cu|| Na half-cells at 2 mA cm^{-2} for 1 mAh cm^{-2}.

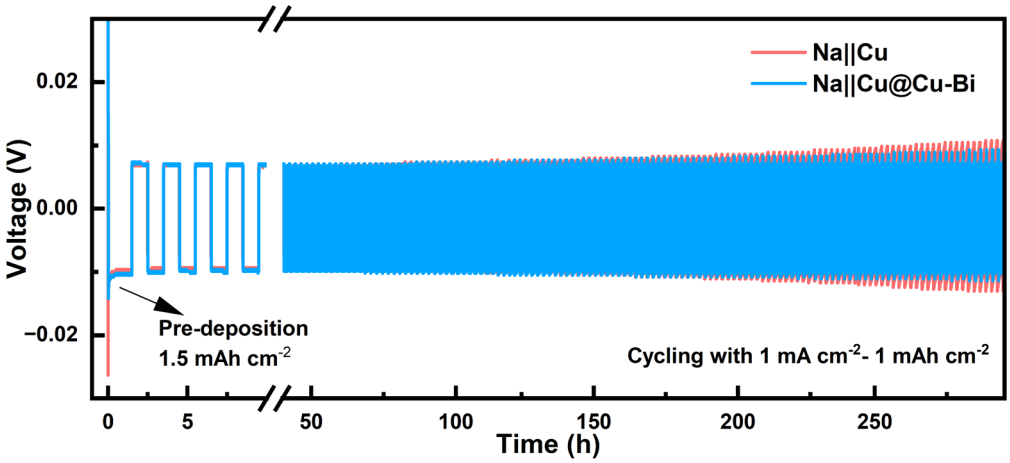

Figure S20. Rate performances of Na||Cu and Na||Cu@Cu-Bi symmetric cells

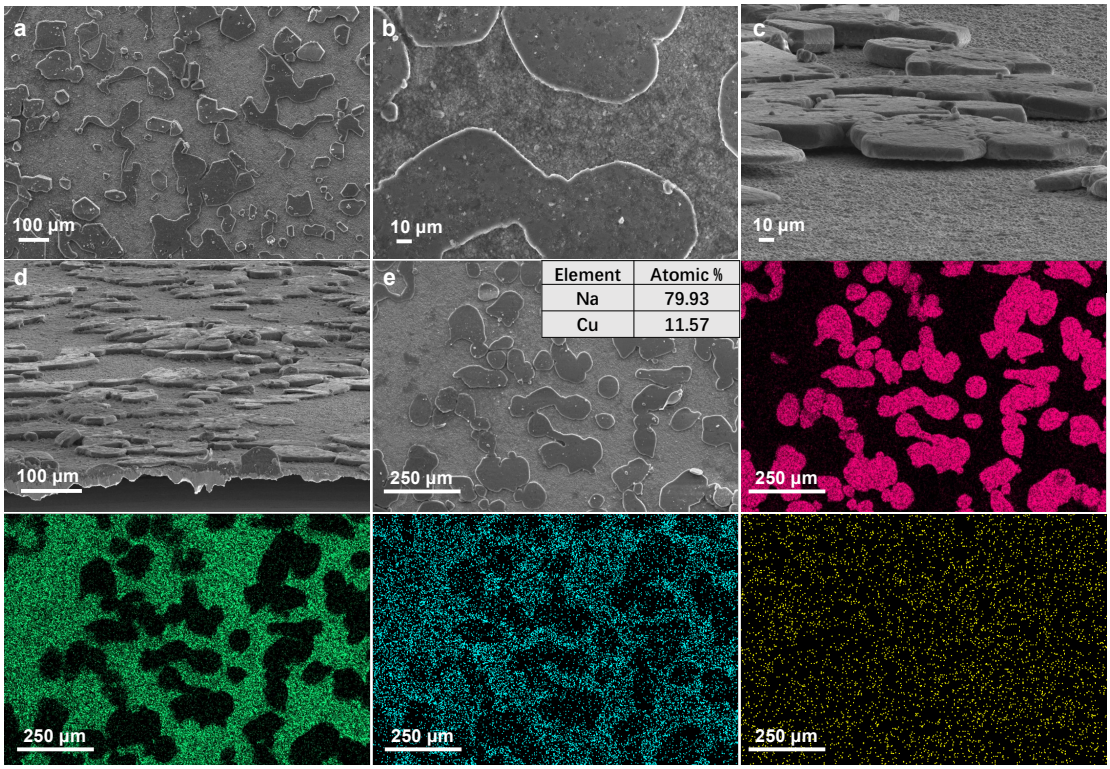

Figure S21. The anode-side SEM images and the corresponding EDS mappings Cu|| NFPP cell in a fully discharged state after 50 cycles at 300 mA g^{-1}.

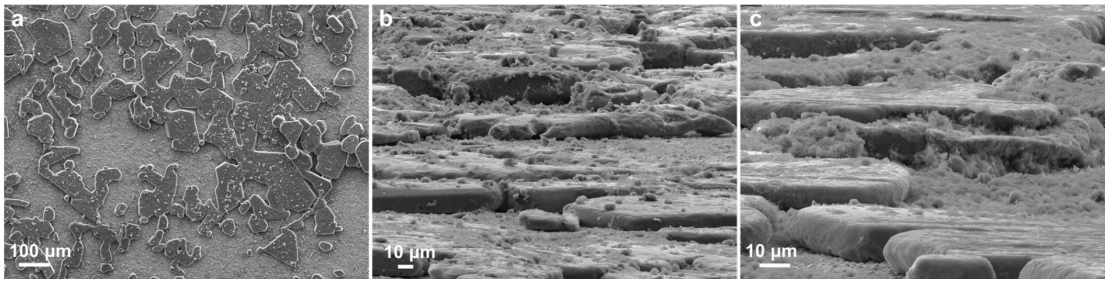

Figure S22. The anode-side SEM images and the corresponding EDS mappings Cu|| NFPP cell in a fully charged state after 50 cycles at 300 mA g^{-1}.

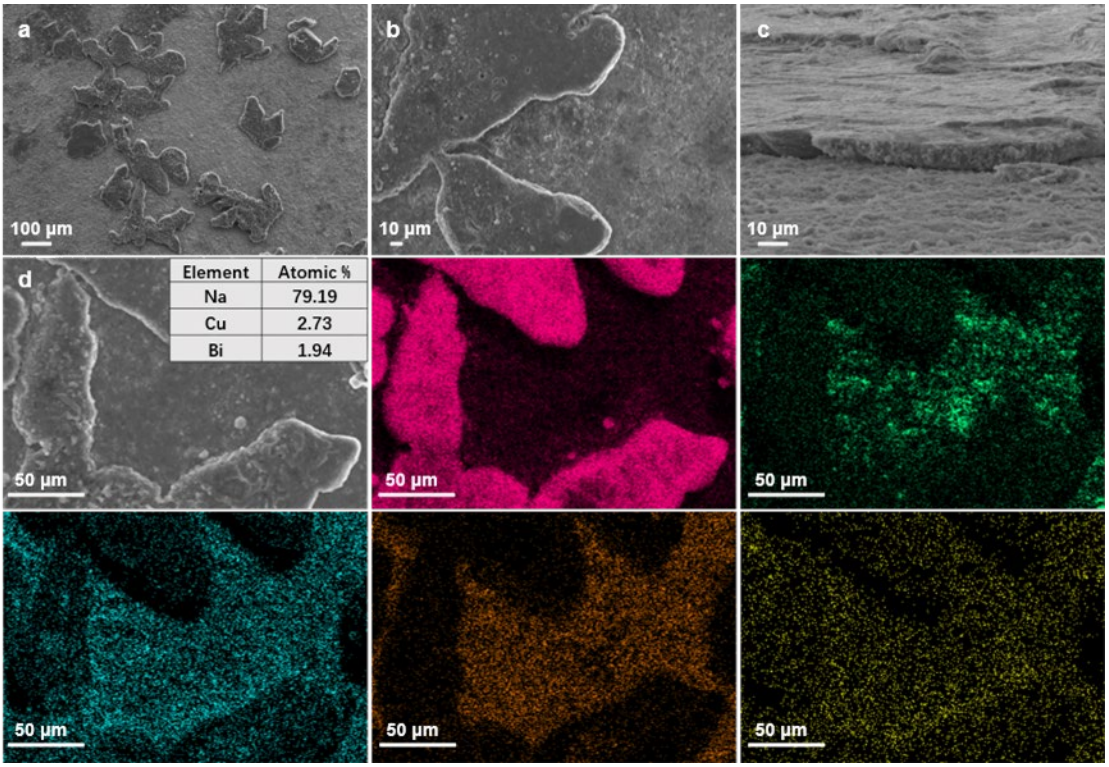

Figure S23. The anode-side SEM images and the corresponding EDS mappings Cu@Bi|| NFPP cell in a fully discharged state after 50 cycles at 300 mA g^{-1}.

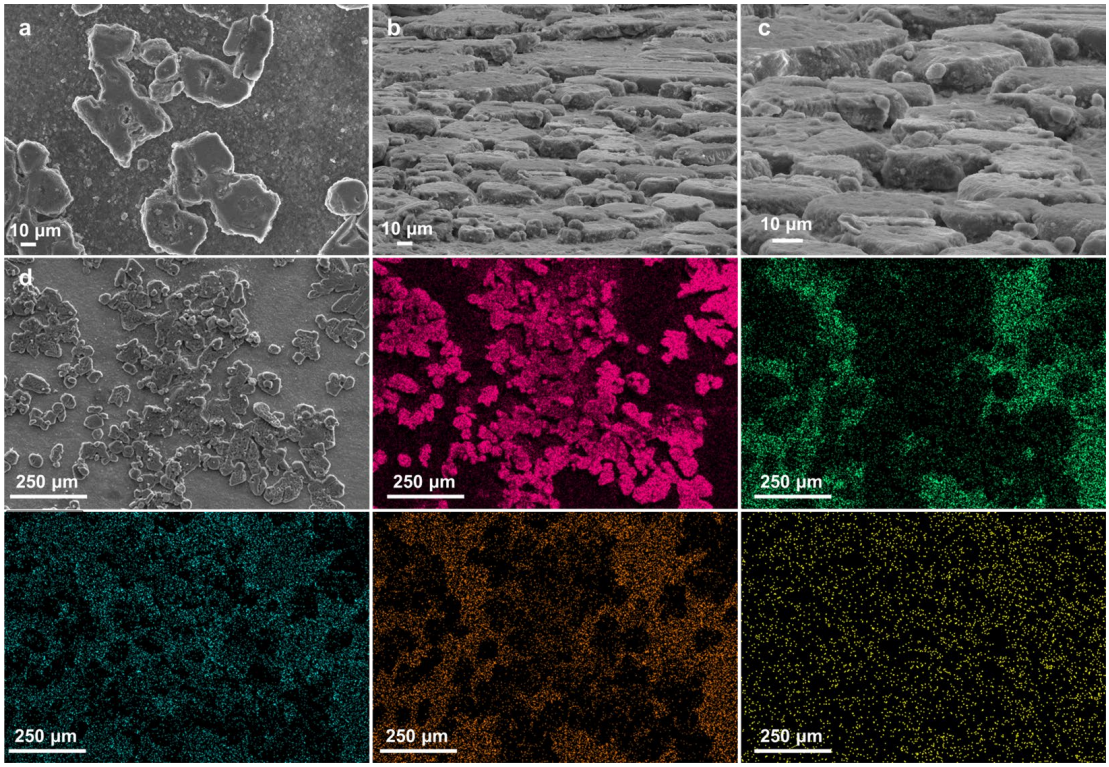

Figure S24. The anode-side SEM images and the corresponding EDS mappings Cu@Bi|| NFPP cell in a fully charged state after 50 cycles at 300 mA g^{-1}.

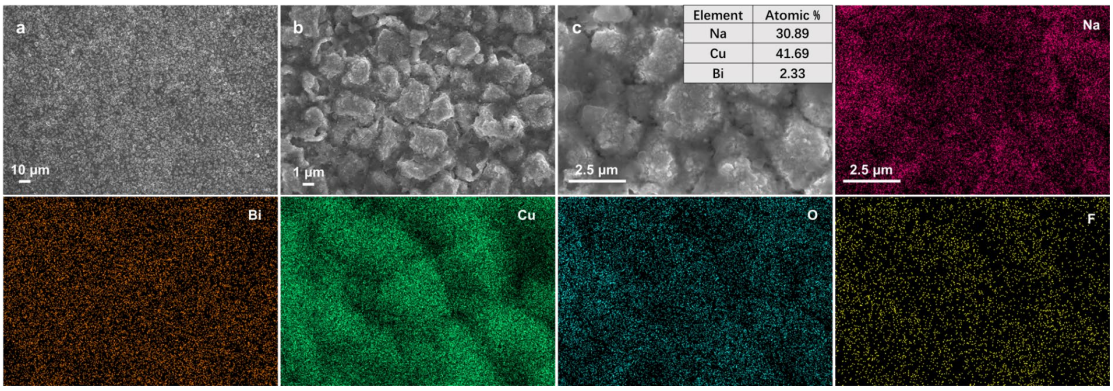

Figure S25. The anode-side SEM images and the corresponding EDS mappings Cu@Cu-Bi ||NFPP cell in a fully discharged state after 50 cycles at 300 mA g^{-1}.

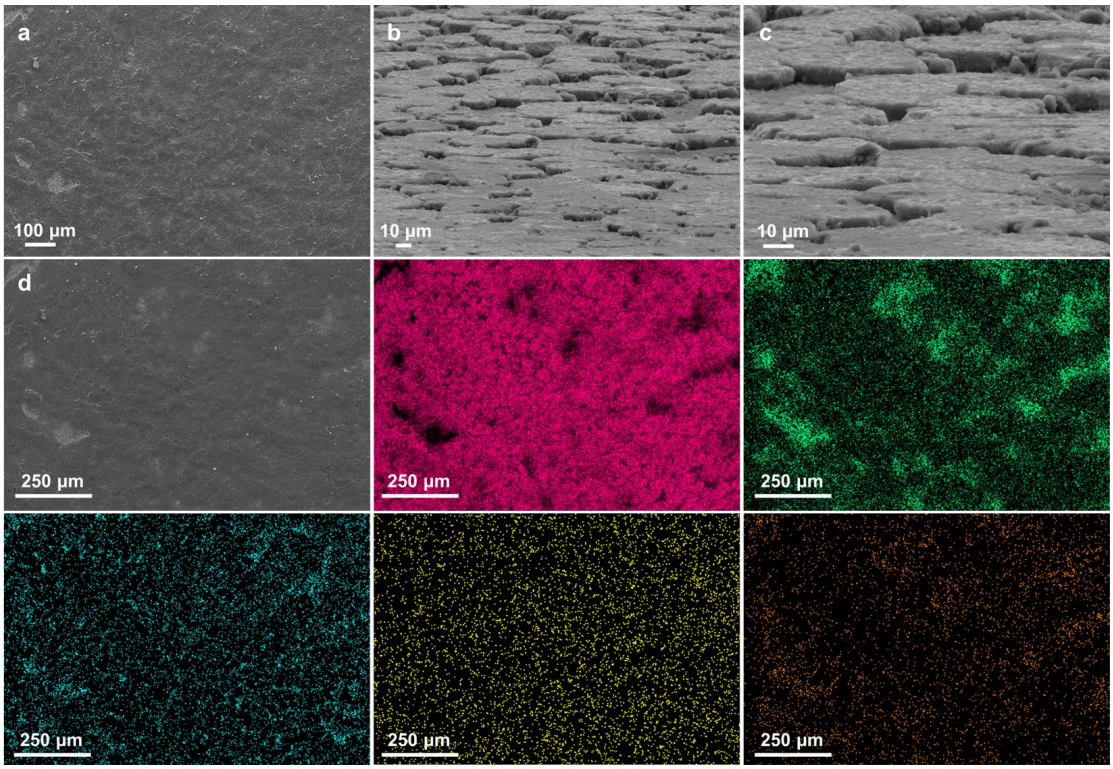

Figure S26. The anode-side SEM images and the corresponding EDS mappings Cu@Cu-Bi|| NFPP cell in a fully charged state after 50 cycles at 300 mA g^{-1}.